

Improved single image dehazing algorithm based on non-local prior

Ling Gan^a, Ziwen Xiong^b

School of Computer Science and Technology, Chongqing University of Posts and Telecommunications,
Chongqing 400065, China

^a16475383@qq.com, ^b291168672@qq.com

Keywords: Image dehazing, Non-local dehazing, L1 regularization, domain transform.

Abstract: The existing single image dehazing algorithm is mostly based on local prior, and the defogging results have problems such as block effect and color distortion. In response to the above problems, an improved algorithm is proposed. Firstly, the non-local prior is used to estimate the initial transmission. Then the L1 regularization method is used to optimize the transmission. The domain transform filter is used to further optimize the transmission to achieve smooth image and suppress noise interference. Simulation results have demonstrated that the improved algorithm can guarantee the readability of a hazed image after removing noise, and the color and the details near the observer in the dehazing image are better than that achieved by the primal method.

1. Introduction

The existing defogging algorithms mainly include two types based on image enhancement methods and physical model based methods. The former method of defogging does not consider the cause of foggy weather degradation, but enhances the visibility of the scene by enhancing the contrast of the image. Moreover, this enhancement generally produces some noise and loss of some information. Image enhancement methods mainly include gray histogram equalization [2], wavelet variation [3], Retinex [4] algorithm and so on. Among them, histogram equalization can improve the contrast of the image, but because the depth of the scene of the foggy image is not uniform, the global histogram equalization can not completely defogging, and some details are still blurred, and some information of the image is often ignored, resulting in image distortion. The latter constructs an atmospheric scattering model, which include partial differential equation method [5], depth-based method [6], prior-based method [7] and so on. He et al. [8] proposed a dark channel priors theory to estimate the transmission by statistical observation of a large number of outdoor fog-free images, but it is easy to produce errors in the sudden change of depth of field, and then use the soft mapping method to refine the transmission and effectively remove the white Halo. Since the method involves the calculation of large-scale sparse matrices, the complexity is high and real-time solution cannot be realized. Later, He et al. [9] used guided filtering instead of soft mapping to improve computational efficiency. Zhu et al. [10] performed statistics on a large number of foggy images, using color attenuation prior to defogging. The algorithm estimates the depth of field map by solving a simple and effective linear model, and then obtains a clear image. However, the color attenuation depends on the color information of the image. The color information at different depths of field has different effects on this prior, so the color attenuation prior is not applicable to the whole fog image.

Most of the above algorithms are based on local pixel blocks for defogging. It is necessary to consider not only the use of multiple block sizes to remove noise interference, but also the problem of block overlap and the block effect in the defogging result. In view of the shortcomings of the above various algorithms, this paper proposes a new improved algorithm. First, the entire image is processed using a non-local prior, and the initial transmission is estimated. The non-local prior considers the global information, and does not need to divide the image into different blocks, which can avoid the halo phenomenon. Secondly, the context-based regularization based on the weighted L1 norm is used to refine the block-based scene transmission to obtain a refined scene transmission.

and then domain transform filtering is used to further optimize transmission.

2. Atmosphere Scattering Model

In computer vision and computer graphics, atmospheric degradation models are widely used in foggy images [11], the model is:

$$I(x) = J(x)t(x) + A[1 - t(x)] \quad (1)$$

Where x denotes the location coordinate of the pixel in the image; $I(x)$ refers to the intensity of the image observed by the camera; $J(x)$ refers to the true intensity of the scene ray; A is the atmospheric light intensity; $t(x)$ is the light transmission of the scene, which can be expressed as

$$t(x) = e^{-\int_{x_0}^x \beta d(x)} \quad (2)$$

Where β is the extinction coefficient. The dehazing method based on the atmospheric degradation model, by estimating the transmission $t(x)$ and the atmospheric light intensity A , and then using the atmospheric degradation model (1) inverse solution to obtain the dehazing image $J(x)$, the inverse solution is

$$J(x) = \frac{I(x) - A}{t(x)} + A \quad (3)$$

In order to avoid the influence of more noise, a lower limit t_0 can be set for t . The last restored image will retain a certain amount of fog in the dense fog area, so that the processed image is more natural, then Eq. (3) can be expressed as

$$J(x) = \frac{I(x) - A}{\max(t(x), t_0)} + A \quad (4)$$

Since I is known, the purpose of defogging is to find the unknown quantities t and A , and then recover the fog-free image J according to Eq. (4).

3. Non Local Prior

Berman et al. [12] clustered the RGB values of a single image in a Berkeley segmentation database (BSDS300) containing various fog-free natural sharp images using the K-means method, and found that a clear and fog-free color image can be used up to a few hundreds of different RGB values to represent (this number is much smaller than the number of pixels of the original image), And different clusters are formed in the RGB space. For a given cluster, the pixels belonging to this cluster are non-local and distributed at different locations throughout the image. Under the influence of fog, the distance between the pixels in different areas of the image is different from the camera. The pixels that originally belong to the same color cluster finally get different RGB values, and are no longer clustered into one cluster, but in RGB space. A line is formed in it, called a fog line.

3.1 Scene Transmission Estimation

The atmospheric light intensity A is estimated using He et al.'s estimation method [9]. Image dehazing based on non-local prior, firstly to obtain the fog line formed by the pixel value clustering of the image, then estimate the transmission, and finally realize image defogging according to the atmospheric physical model.

3.1.1 Finding Haze-Lines

According to the previously estimated atmospheric light A , the color distance from the pixel point on the fog line to the atmospheric light can be defined as:

$$I_A(x) = I(x) - A \quad (5)$$

Following Eq. (1),

$$I_A(x) = t(x) \bullet [J(x) - A] \quad (6)$$

$I_A(x)$ is expressed in the spherical coordinate system as:

$$I_A(x) = [r(x) \ \theta(x) \ \varphi(x)] \quad (7)$$

Taking atmospheric light A as the center of the sphere, $r(x)$ is the distance from the pixel point to the center of the sphere.

$$r(x) = \|I(x) - A\| \quad (8)$$

Where $\theta(x)$ and $\varphi(x)$ represent longitude and latitude, respectively.

It can be seen from equation (6) that for a given J and A , scenes at different depths of field differ only in the value of t . Assuming that $\theta(x)$ and $\varphi(x)$ are not changed, the change in t is only related to the change in $r(x)$.

In the fog-free image, if the longitude θ of the pixel point x and the pixel point y are the same as the latitude φ , they have similar RGB values as follows

$$J(x) \approx J(y) \Rightarrow [\varphi(x) \approx \varphi(y), \theta(x) \approx \theta(y)] \quad (9)$$

Therefore, the pixel points with the same θ and φ belong to the same fog line.

The k-d tree is used to cluster the longitude θ and the latitude φ of the pixel points in the figure to determine whether the pixels belong to the same fog line.

3.1.2 Estimating Initial Transmission

After the fog line corresponding to the pixel point is obtained by clustering, the transmittance t can be initially estimated based on the aforementioned analysis. For a fog line defined by J and A , according to equations (1) and (8):

$$r(x) = t(x) \|J(x) - A\| \quad (10)$$

Where $0 \leq t(x) \leq 1$, then when $t(x)=1$, the corresponding maximum distance radius r_{\max} is

$$r_m = \|J(x) - A\| \quad (11)$$

According to equations (10) and (11), the transmittance $t(x)$ is defined as

$$t(x) = \frac{r(x)}{r_m} \quad (12)$$

The position where r is the largest on a fog line is the position of the pixel point that is least affected by the fog. Assuming that the fog line H contains a fog-free pixel, the maximum distance r_{\max} of this fog line is defined as

$$\hat{r}_m = \max_{x \in H} [r(x)] \quad (13)$$

According to equations (12) and (13), the transmission based on a single pixel point estimate

$$\tilde{t}(x) = \frac{r(x)}{\hat{r}_m} \quad (14)$$

4. Proposed Method

The image dehazing algorithm based on prior theory is generally divided into four steps: estimation of atmospheric light value, estimation of atmospheric transmission, optimization of

transmission map, and solution of atmospheric degradation model. This paper mainly improves and optimizes the transmission optimization, and proposes an improved non-local defogging algorithm, such as fig.1:

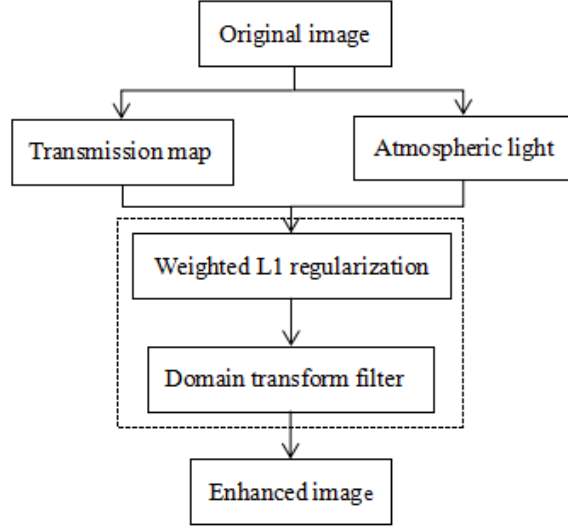


Fig.1 The framework of our dehazing method

4.1 Weighted L1 Regularization

To avoid the disadvantages of current non-local dehazing methods, it does not consider the relationship between neighboring pixels, this paper is inspired by the MENG [13]. The relationship between the transmission and the depth of field is expressed by the equation (2). In a small local region, pixels in the same depth of field should have similar transmission, use the color difference of adjacent pixels to construct weights. The function $W(x, y)$ causes the difference in transmission between two adjacent pixels at the same depth of field to be zero, which satisfies

$$w(x, y) \{t(y) - t(x)\} = 0 \quad (15)$$

Where x and y are two adjacent pixels, the difference in transmission is adjusted by the constructed weight function, and a smaller $W(x, y)$ is selected when the depth variation is larger, and vice versa. Obtaining depth information of an image is difficult. It is assumed here that if the color difference of adjacent pixels is smaller, the two pixels have the same depth information, and vice versa. The expression of the weight is

$$w(x, y) = e^{-\|I(x) - I(y)\|^2 / 2\delta^2} \quad (16)$$

Where $\|I(x) - I(y)\|$ represents the pixel difference between two adjacent pixels, and the edge detection operator can reflect the gradient change of the image. Here, the Kirsch edge detection operator pair of eight template directions is used to equation(16) do the convolution operation, the final weighting function is

$$w_j(i) = \exp\left(-\sum_{c \in \{r, g, b\}} \|(D_j \otimes I^c)_i\|^2 / 2\delta^2\right) \quad (17)$$

The total weight of L1 regularization

$$\sum_{j \in w} \|w_j \bullet (D_j \otimes t)\|_1 \quad (18)$$

Where D_j is a set of Kirsch operators, i represents the index of the i -th weighting function of the j -th filter construction, where $i=1, 2, \dots, 8$, the parameter δ is the standard deviation.

Through the above analysis, the $\sum_{j \in w} \|W_j \cdot (D_j t)\|_1$ norm-constrained transmission is introduced,

and the constraint equilibrium is added to optimize the relationship between the primary transmission and the optimized transmission by minimizing the following cost loss function

$$\theta \|t - t_y\|_2^2 + \sum_{j \in w} \|w_j \bullet (D_j \otimes t)\|_1 \quad (19)$$

Where the first part is the data term, the optimized transmission image should be close to the primary transmission, the second part models the contextual constraints of $t(x)$, and θ is the regularization parameter for balancing the two terms. Direct minimization (19) has great difficulty. MENG et al. use variable splitting method to introduce auxiliary variable μ_j to construct a new cost function.

$$\theta \|t - t_y\|_2^2 + \mu \left(\sum_{j \in w} \|\mu_j - (D_j \otimes t)\|_2^2 \right) + \sum_{j \in w} \|w_j \bullet \mu_j\|_1 \quad (20)$$

Finally, by obtaining the partial derivative function of equation (20) and making the partial derivative function zero, the optimized transmission t_y is finally solved. We iteratively increase u from $u_0 = 1$ to $u_{\max} = 2^8$ by a scaling factor $2\sqrt{2}$.

4.2 Optimized Based on Domain Transform Filter

The edge-preserving filtering[14] effect based on domain transform ensures the smoothing and edge-preserving characteristics. The domain transformation requires only one-dimensional filtering in the transformed domain space, which greatly reduces the filtering time. The core of the algorithm lies in Looking for a domain transformation mapping function that keeps the original image spatial and range information unchanged, so that the image can be processed with simple one-dimensional filtering in the new domain. The main process formula for domain transform filtering to optimize transmission can be expressed as:

$$t(u) = \int_1^u \frac{\sigma_H}{\sigma_S} + \frac{\sigma_H}{\sigma_r} \sum_{k=1}^c |I'_k(x)| d_x \quad (21)$$

Where I_k represents the K -th channel of the input image I , σ_H can artificially specify the standard deviation of the filter kernel, which is a free parameter, so that $\sigma_H = \sigma_S$ can be obtained, thus obtaining the formula

$$t(u) = \int_1^u 1 + \frac{\sigma_s}{\sigma_r} \sum_{k=1}^c |I'_k(x)| d_x \quad (22)$$

One-time processing of all channels of the input image is an important factor for edge-preserving filtering. This formula converts the multi-channel of the input image into one-dimensional space at one time, ensuring that more input images can be used in the subsequent filtering process of the transform domain. Simultaneous processing of the channels avoids the problem of introducing artifacts at the edges.

5. Experiment and Analysis

The experiment hardware platform was: Intel(R) Core(TM) i5-4200 CPU @ 1.60GHz 2.30GHz; 4.00GB for ARM; The software platform was: MATLAB R2016a 64-bit. All the algorithms were implemented using MATLAB code.

5.1 Experiments Using the FRIDA Dataset

The proposed algorithm is evaluated on the dataset, namely FRIDA. The results of the algorithm presented on the FRIDA dataset demonstrate the method's ability to handle difficult scenarios such as heterogeneous fog and clouds. Structural similarity (SSIM)[15] and peak signal to noise ratio (PSNR)[16] were used to evaluate the performance of dehazing.

The smaller the value of SSIM, the better the structural information of the defogged image is saved. The larger the PSNR value, the smaller the distortion of the image relative to the original image after defogging, and the better the defogging effect.

The experimental results of SSIM and PSNR are shown in Table 1. In the column of SSIM, the SSIM value of the algorithm is smaller than that of the other four methods, which proves that our improved dehazing algorithm can change the information of retained structure. Similarly, the PSNR value in the PSNR column is larger than the values of the other four methods, which proves that the smaller the distortion of the image relative to the original image after defogging, the better the defogging effect.

Table 1 SSIM and PSNR comparison

Method	Parameter	
	SSIM	PSNR
Method from [18]	0.6594	70.6638
Method from [10]	0.6962	68.9526
Original algorithm [12]	0.6789	69.8825
Method from [19]	0.7188	66.7285
Proposed	0.6583	71.7650

In order to further verify the effectiveness of the proposed algorithm, three objective evaluations are used to illustrate the algorithm. The non-reference image quality evaluation method often used in the image dehazing field [17], through the visible edge set number e , the average gradient r , the percentage of saturated pixels σ as the evaluation index. Among them, the larger the values of e and r , the smaller percentage of saturated pixels σ , the better the dehazing effect of the algorithm.

Table 2 indicates that the proposed algorithm scores best in terms of percentage of saturated pixels σ , and average gradient r . Explained it can better maintain the brightness and color of original image scene, especially in near scene; there is no over-saturation phenomenon in distant highlights in defogging image.

Table 2 Proposed results on FRIDA dataset.

Method	Parameter		
	e	δ	r
Method from [18]	1.65	0.00	1.33
Method from [10]	1.38	0.00	1.92
Original algorithm [12]	0.41	0.00	1.54
Method from [19]	1.76	0.01	1.78
Proposed	1.50	0.00	2.12

5.2 Experiments on the global image dataset

Fig.3 provides a comparison of the images restored from smoggy images by the two algorithms, which have different atmosphere light estimation rationales. As is evident from this figure and the table 3, relative to the old algorithm the proposed one produces effects that look more natural. The results obtained from the three evaluation indexes are mostly optimal.



Fig.3 Comparison of Defogging Result. From left to right: Original image, result of original algorithm [12], result of proposed algorithm.

Table 3 Comparison with the original algorithm

Image	Original algorithm[12]			Proposed algorithm		
	e	δ	r	e	δ	r
Forest	0.254	0.003	1.740	0.239	0.006	1.706
Sweden	0.317	0.000	2.126	0.365	0.001	2.174
Manhattan	-0.050	0.030	1.829	-0.051	0.035	1.804

6. Conclusion

In this paper, the non-local dehazing algorithm is improved by Weighted L1 regularization. Domain transform filtering refines the transmission to preserve edge details better. In our future works, texture and other features will be jointly employed. In addition, the brightness will be reformed. Then the dehazed images can be more realistic. Moreover, we have examined the improved method with five objective indexes. Compared with other four methods, the improved method also achieved higher PSNR and SSIM values, at the same time, there are also good values on the other three evaluation indicators. thus, leading to a better recovery quality.

Reference

- [1] Wang R , Li R , Lian X Q . Multiple Scattering Model Based ImageDehazingwith Superpixel[J]. Guangzi Xuebao/Acta Photonica Sinica, 2016, 45(4): 0410002.
- [2] Ibrahim H , Kong N S P . Brightness Preserving Dynamic Histogram Equalization for Image Contrast Enhancement [J]. IEEE Transactions on Consumer Electronics, 2008, 53(4):1752-1758.

- [3] Ping W , Chun Z , Ying-Xin L . Fast algorithm to enhance contrast of fog-degraded images[J]. Journal of Computer Applications, 2006, 26(1):152-154.
- [4] Jobson D J , Rahman Z , Woodell G A . A multiscale retinex for bridging the gap between color images and the human observation of scenes[J]. IEEE Transactions on Image Processing, 1997, 6(7):965-976.
- [5] Sun Y , Xiao L , Wei Z et al. Method of defogging image of outdoor scenes based on PDE. J Syst Simulation, 2007, 19(16):3739-3744.
- [6] Zhang S , Qing C , Xu X , et al. Dehazing with improved heterogeneous atmosphere light estimation and a nonlinear color attenuation prior model[C]// International Symposium on Communication Systems. IEEE, 2016,p.1-6.
- [7] Jiexian Z , Yonglong Y . Image defogging and edge preserving algorithm based on dark channel prior and bilateral filtering[J]. Journal of Image and Graphics, 2017, 22(2):147-153.
- [8] He K , Sun J , Fellow, et al. Single Image Haze Removal Using Dark Channel Prior[J]. IEEE Transactions on Pattern Analysis and Machine Intelligence, 2011, 33(12):2341-2353.
- [9] HE K, SUN J, TANG X O. Guided image filtering[J]. IEEE transactions on pattern analysis and machine intelligence, 2013,35(6) : 1397-1409.
- [10] Zhu Q , Mai J , Shao L . A Fast Single Image Haze Removal Algorithm Using Color Attenuation Prior [J]. IEEE Transactions on Image Processing, 2015, 24(11):3522-3533.
- [11] Narasimhan S G , Nayar S K . Vision and the Atmosphere [J]. International Journal of Computer Vision, 2002, 48(3):233-254.
- [12] Berman D , Treibitz T , Avidan S . Non-local Image Dehazing[C].IEEE Conference on Computer Vision and Pattern Recognition, 2016:1674-1682.
- [13] Meng G , Wang Y , Duan J , et al. Efficient image dehazing with boundary constraint and contextual regularization[J]. In: Proceedings of IEEE 16th International Conference on Computer Vision. 2013: 617~624.
- [14] Gastal E S L , Oliveira M M . Domain transform for edge-aware image and video processing [J]. ACM Transactions on Graphics, 2011, 30(4):1.
- [15] Wang Z , Bovik A C , Sheikh H R , et al. Image Quality Assessment: From Error Visibility to Structural Similarity[J]. IEEE Transactions on Image Processing, 2004, 13(4).
- [16] Hore A , Ziou D. Image Quality Metrics: PSNR vs. SSIM[J]. 2010:2366-2369.
- [17] Hautiere N , Tarel J P , Aubert D , et al. Blind contrast enhancement assessment by gradient ratioing at visible edges.(Report)[J]. Image Analysis & Stereology, 2011, 27(2):87-95.
- [18] J.-P. Tarel , N. Hautiere , Fast visibility restoration from a single color or gray level image, in: 2009 IEEE 12th International Conference on Computer Vision, IEEE, 2009, pp. 2201 - 2208 .
- [19] Zhu M , He B , Wu Q . Single Image Dehazing Based on Dark Channel Prior and Energy Minimization [J]. IEEE Signal Processing Letters, 2017, PP(99):1-1.